Egypt. J. Chem. **Vol. 65,** No. 10 pp. 447 - 454 (2022)

Egyptian Journal of Chemistry

http://ejchem.journals.ekb.eg/

Graft Co-Polymer Nano Particle as Carbon Steel Corrosion Inhibitor in 1M H_2SO_4 At 293K

Hamida. I. Salman[1], Mohammed. N. Bahjat[1], Doaa. R. Mohammedali[*1], Emad Salaam Abood[2]

[1]Chemistry Department, College of Education for Pure Sciences, University of Kerbala, Kerbala/ Iraq

[2] Medical physics department, Hilla University College, Babylon, Iraq

Abstract

New graft co-polymer nano-particle (coating nano-polymer) was prepared as a corrosion inhibitor in 1M sulfuric acid. The synthesized coating nano-polymer was characterized by FT-IR, ^{1}H NMR and atomic force microscope (AFM). Synthesized coating nano-polymer mixed with acrylic acid in different proportion (0.2-0.8 mole: 293K: 30 min). Potential-dynamic polarization technique is used to get current corrosion, inhibition efficiency, cathodic and anodic Tafel slopes with examination of concentration influence on inhibition efficiency, the results revealed that the inhibition efficiency increases as inhibitor concentration increases. The maximum inhibition recorded efficiency 93% at 0.8 mol.

Keyword: Corrosion; Carbon Steel; graft co-polymer nano partical; Inhibitor; Coating; alloy; adsorption.

1. Introduction

Corrosion is a gradual destruction of materials and change of refined metal into a more chemically stable oxide by chemical or electrochemical reaction with surrounding environment. Also, it occurs to other materials such as polymers and ceramic. The circumstances of corrosion occurrence are cathode reduction electrode, anode oxidation electrode and electrolyte solution that has metal [1-3]. It corrodes due to redox reaction, at which charge transfers between an electronic conductor (metal) and an ionic conductor (aqueous solution) occur. Also, the study of corrosion phenomena requires knowledge of the chemical and kinetic balances involved in these reactions. In addition to electrochemical reactions, aqueous corrosion involves surface reactions (adsorption) as well as acid-base reactions, in particular the hydrolysis of metal cations (Fe^{2+} to Fe $(OH)_2$).[4]

Effective corrosion inhibition has a high economic value as the annual corrosion cost due to it destroys more than three per cent of the world's GDP.[5] So it is very necessary to find appropriate ways to protect metals from corrosion[6, 7]. Many financial and economic efforts are spent annually to overcome corrosion phenomenon to minimize of its effect of metals damage, changes in metal properties, loss of material and environmental and human damage.[8, 9]

Carbon steel is one of the commonly used metals in industry and engineering applications [10] such as manufacture of parts for marine and land transportation as it has good mechanical properties.[4] Carbon steels, which are less expensive than corrosion-resistant alloys, are widely employed as the preferred construction material in a variety of industries. Carbon steels typically have a carbon content of less than 1.5 percent, with minor amounts of Mn, Si, P, and S. Low carbon steels (0.25% C), medium carbon steels (0.25–0.70 percent C), and high carbon steels (0.70–1.05 percent C) are classified based on carbon content. The amount of carbon in a material can be changed to achieve varied mechanical qualities including strength, ductility, and hardness. [10]

Nowadays, awareness of corrosion protection has increased, as study inhibitory effect of organic compounds and plant extracts with using of coating in different corrosion environments.[11, 12] Protection to prevent or control corrosion of metal corrosion is used via using inhibitors in low concentration that can be chemical or natural, organic or inorganic.[13-16]

Organic polymer coatings have received significant attention in corrosion prevention, due to their ease of application, sticking strongly to each other due to the presence of different metal ions which form complexes with them, and they also absorb well on

*Corresponding author e-mail: doaa.r@s.uokerbala.edu.iq.; (Doaa. R. Mohammedali).

Receive Date: 16 May 2022, Revise Date: 29 May 2022, Accept Date: 31 May 2022

DOI: 10.21608/EJCHEM.2022.138851.6103

metal surfaces, all of that can protect the metal from corrosion [17-23]

Based on this survey, our aim of this work is to prepare a friendly environmental, less expensive, a high molecular weight Nano-Polymer, and contains conjugated double bond with hydroxyl group as corrosion-resistant barrier [24-27]. Also, test this new synthesized Nano-Polymer as coating to carbon steel to control corrosion.

Experimental

*General***:** All chemicals were purchased from different companies and used without purification and electrochemical measurements were performed on MLab 200 Potentiostat/Galvanostat.

Synthesis of graft PTGM Nano-particles:

332.26g terephthalic acid (2.0 mol) dissolved in 50 ml DMSO were added to two-necked round bottom flask that equipped with a thermometer. The mixture warmed carefully at 40ºC with stirring until clear liquor is formed then add 92g of glycerol (1.0 mol) with continues heating at 120ºC. 25 mL p-Xylene were added carefully to the reaction, in the form of batch (two drops in each batch), as dehydrating agent, with continues heating to 80 min at 145ºC. Leave the reaction flask to cool to about 50ºC.

58g maleic anhydride (0.5mol) in 10 ml o DMSO at 40ºC was added to reaction mixture with rising heat to 90ºC. Dehydrating agent of p-Xylene (two drops in each batch) was added with rising heat to 105ºC for 40 min. The reaction mixture left to cool, add cold distilled water, leave the suspension overnight, filter and wash with distilled water and leaves to dry over suction to get graft PTGM Nano-particles (Scheme 1).

Preparation of carbon steel specimens

Cylindrical shaped carbon steel was designed (2.5 cm diameter and 3 mm height) and its chemical composition is 0.462% C, 0.260% Si, 0.597% Mn,0.0108% P, 0.0215% S, 0.0877% Cr, 0.0206% Mo, 0.0974% Ni, 0.0275% Al, 0.297% Cu and Fe balanced. The sample was grounded with emery cloth (grade 80–400), washed, dried and stored until use (Figure 1).

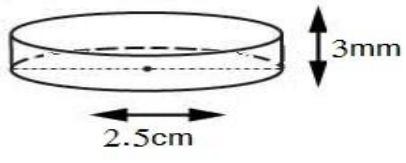

Figure 1: schematic diagram of carbon steel specimen

Preparation of coating:

Nano-Polymer (0.1 g, 1.168 * 10^{-4} mol) mixed with acrylic acid (various moles: 0.2, 0.4, 0.6, 0.8, 1 mol), with addition of 2-3 drops of cobalt octoate as drier and hardener with continuous mixing until getting an orange solution. This orange solution is used as coating layer to carbon steel samples wait to dry (Figure 2).

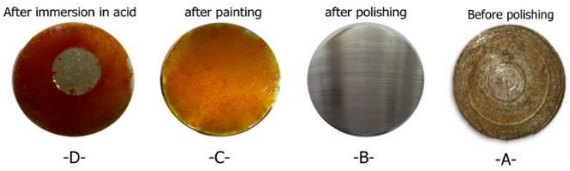

Figure 2: Surface of carbon steel samples

Preparation of Corrosive environment solutions:

The attacker solution 1M H_2SO_4 was prepared through mitigation of analytical degree 98% H_2SO_4 solution with distilled water.

Potentiostatic Polarization Measurements:

Potentiostatic polarization measurements were conducted in a cell consists of three electrodes, reference electrode (calomel electrode RE), auxiliary electrode (platinum electrode AE), and working electrode (carbon steel samples WE). The working electrode was dipped into the test solution for 30 min, with a time step of 1 sec and left to attain steady-state open circuit potential (OCP). Potential range was auto (±250 mv) relative to the OCP. The corrosion potential (E_{corr}) and corrosion current density (I_{corr}) were measured by tafel method. The inhibition efficiency (Ƞ%) was calculated as in equation (1).[28]

$$Ƞ\% = \frac{I_{corr} - I_{inh}}{I_{corr}} \times 100\ \% \quad \ldots\ldots\ldots\ldots\ldots (1)$$

Where Ƞ% is the ratio of the efficiency of inhibition. I_{corr} , I_{inh} is corrosion current density in the absence and presence of inhibitors.

3. Results and Discussion

3.1. Preparation of graft co-polymer:

Terphthalic acid reacted with glycerol at reflux temperature for 80 min to afford linear nano copolymer which is used in the next step as initiator to react with malic anhydride for 40 min at 105ºC to afford Poly(Terphthalic acid-Co-Glycerol-G-Maleic anhydride) (PTGM Nano Particle) as final desired product (Scheme 1). [29, 30]

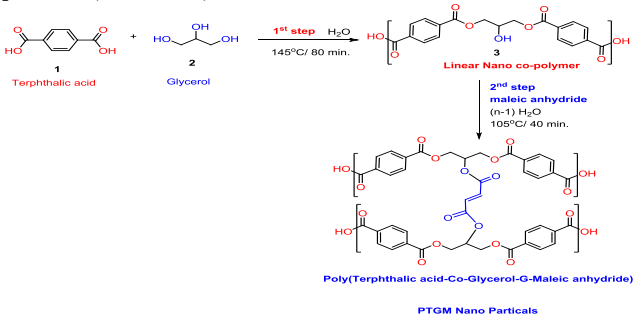

Scheme 1: Synthesis of PTGM Nano Particles

The structure of new compounds; linear nano copolymer and PTGM Nano Particle were confirmed via using FT–IR and 1HNMR. IR (KBr) spectrum of linear nano copolymer revealed presence of alcoholic OH at 3423 cm^{-1}, 2544 cm^{-1}, 2654 cm^{-1} related to C-H $sp^3$and sp^2hybridization, 1726 cm^{-1} of ester C=O, 1597, 1581 cm^{-1} of aromatic C=C, and 1284 – 1259cm^{-1} that related to C-O absorption band (Figure).

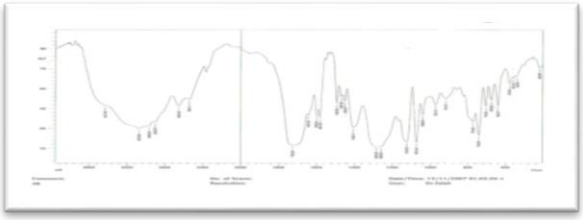

Figure 3: The FT-IR spectrum of linear co-polymer

Also, ^{1}HNMR of the liner co-polymer revealed presence of signals at δ 7.53- 8.10 ppm as multiples that related to aromatic protons, δ 6.27-6. 46 ppm of methine protons, δ 4.24- 4.50 ppm of CH_2 protons, and at δ 3.44- 3.62 ppm that related to aliphatic alcohol together with characteristic signals of alcoholic OH at δ 13.24 ppm as singlet signal which exchangeable with D_2O (Figure 3).

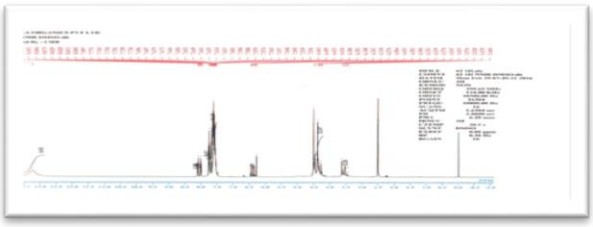

Figure 4: The ^{1}HNMR spectrum of linear co-polymer

In the same manner, FT–IR (KBr) spectrum of the graft co-polymer revealed significant peaks at 3500 cm^{-1} which related to alcoholic OH, at 2880 cm^{-1} , 3140 cm^{-1} and 3050 cm^{-1} of aliphatic C-H, aromatic =C-H and alkenes =C–H, respectively. Also, strong sharp band at 1740 cm^{-1} and 1250 cm^{-1} that related to ester C=O ester and C-O, respectively (Figure 5).

Table (4) , Fig (6), The spectrum of ^{1}HNMR (600 MHz, (CD3)3SO) of the graft co-polymer

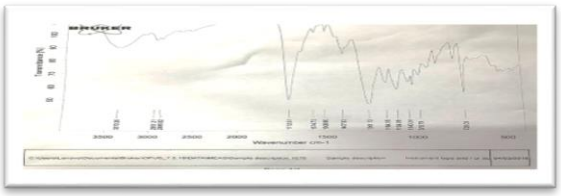

Figure 5: FT-IR spectrum of graft co-polymer

Besides, The spectrum of ^{1}HNMR (600 MHz, $(CD_3)_3SO$) of the graft co-polymer have signals at 13.12ppm of carboxylic OH, 7.79 and 7.48 ppm that related to methane of CH=CH, while at 4.28-4.23 as doublet is related to methylene protons (Figure 6).

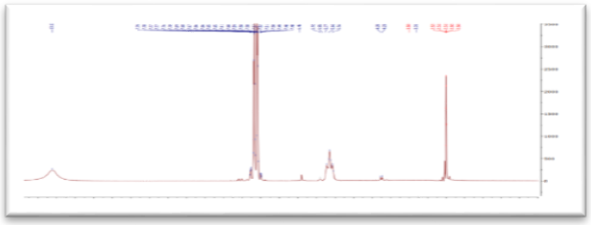

Figure 6: The ^{1}HNMR spectrum of graft co-polymer

The size of particles were measured by the atomic force microscope (AFM); that revealed that outer surface of the nanoparticles of linear co-polymer (Figure 7). The roughness of this surface and the square root square are calculated according to the coefficient:

$$Rm \sqrt{\sum_{i=1}^{n} \frac{(Zi - Zav)^2}{N}}$$

Where N, Z = the number of measured points

The roughness coefficient of a linear co-polymer surface was 1.19 nm and the square root square was equal to 1.37 nm. This indicates that the bold size of the nanoparticles plays an important role in the roughness of the surface, its uniform crystalline system, and the surface homogeneity, Also, the average of height of the particles was equal to 4.80 nm (Figure 7a).

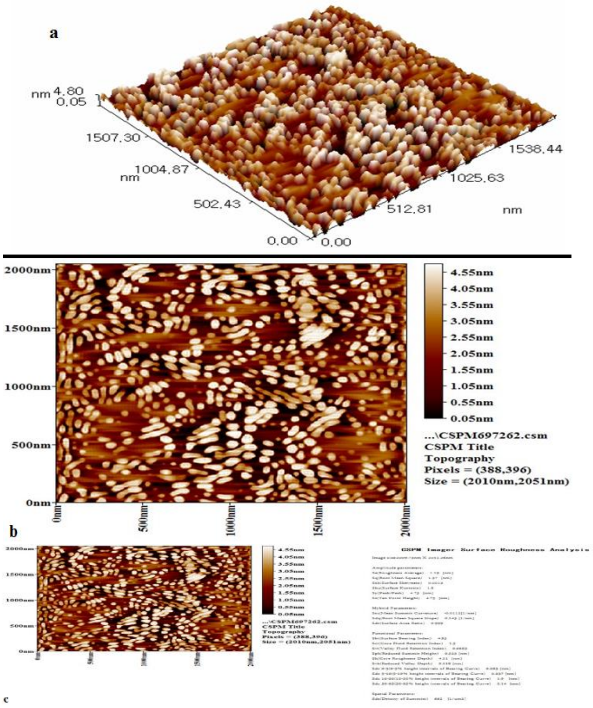

Figure 7: outer surface of the nanoparticles of linear co-polymer a) 3D Image, b) 2D Image, c) 2D Image with particle details.

Table 1 represents the total rate of the particle sizes of the common linear nanoparticle and the different proportions of these volumes; the results indicate that

the molecular size of the linear co-polymer nanoparticle was 94.09 nm. Also, Figure 8 represents the distribution of the different proportions of particle sizes of the linear co-polymer nanoparticle. On the other hand, Fig (9 a, b &c) shows the outer surface of the nanoparticles of graft co-polymer.

The roughness coefficient of a graft co-polymer surface was 2.12 nm and the square root square was equal to 2.44 nm. This indicates that the bold size of the nanoparticles plays an important role in the roughness of the surface, its uniform crystalline system, and the surface homogeneity, Also, the average of height of the particles was equal to 8.3 nm, as observe in Fig (9 a).

Table (2) represents the total rate of the particle sizes of the graft co-polymer nanoparticle and the different proportions of these volumes; the results indicate that the molecular size of the graft co-polymer nanoparticle was 74.39 nm and fig (10) represent the distribution of the different proportions of particle sizes of the graft co-polymer nanoparticle.[31, 32]

Table (1): The total rate of the particle sizes of the linear co-polymer nanoparticle and the different proportions of these volumes

Sample:1 **Code:** Sample Code
Line No.: lineno **Grain No.:**139
Instrument: CSPM **Date:**2018-04-23
Avg. Diameter: 94.09 nm **<=10% Diameter:**75.00 nm
<=50% Diameter: 90.00 nm **<=90% Diameter:**115.00 nm

Diameter (nm)<	Volume (%)	Cumulation (%)	Diameter (nm)<	Volume (%)	Cumulation (%)	Diameter (nm)<	Volume (%)	Cumulation (%)
75.00	7.19	7.19	100.00	8.63	68.35	125.00	1.44	93.53
80.00	12.95	20.14	105.00	7.19	75.54	130.00	5.76	99.28
85.00	16.55	36.69	110.00	7.19	82.73	145.00	0.72	100.00
90.00	11.51	48.20	115.00	5.04	87.77			
95.00	11.51	59.71	120.00	4.32	92.09			

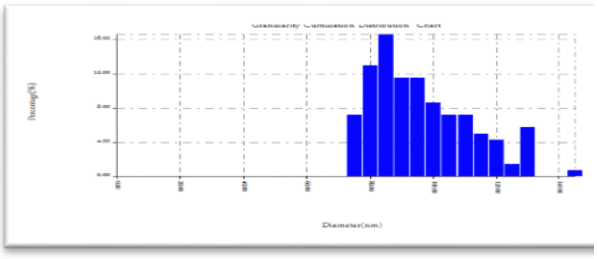

Figure 8: Distribution of the different proportions of particle sizes of the linear co-polymer nanoparticle.

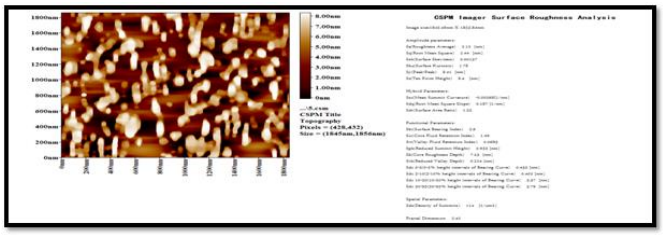

Figure 9: The outer surface of the nanoparticles of graft co-polymer
a) 3D Image, b) 2D Image, c): 2D Image and showing all details of particles.

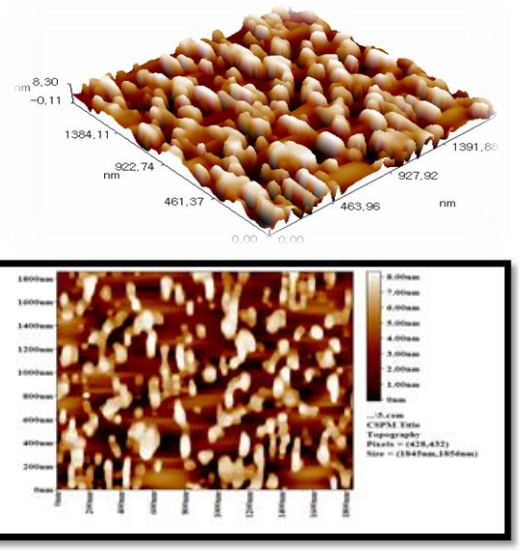

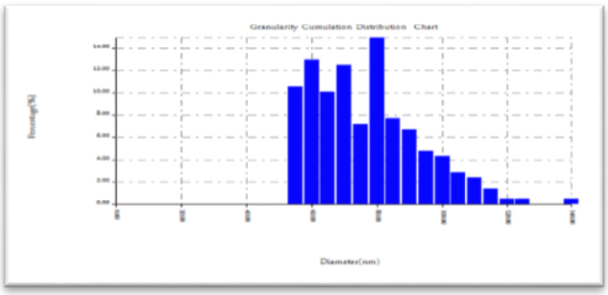

Figure 10: Distribution of the different proportions of particle sizes of the graft co-polymer nano particle.

Table (2): The total rate of the particle sizes of the graft co-polymer nanoparticle and the different proportions of these volumes

Sample:2 **Code:** Sample Code
Line No.: lineno **Grain No.:**208
Instrument: CSPM **Date:** 2019-05-31
Avg. Diameter:74.39 nm **<=10% Diameter:0 nm**
<=50% Diameter:70.00 nm **<=90% Diameter:95.00 nm**

Diameter (nm)<	Volume (%)	Cumulation (%)	Diameter (nm)<	Volume (%)	Cumulation (%)	Diameter (nm)<	Volume (%)	Cumulation (%)
55.00	10.58	10.58	85.00	7.69	75.96	115.00	1.44	98.56
60.00	12.98	23.56	90.00	6.73	82.69	120.00	0.48	99.04
65.00	10.10	33.65	95.00	4.81	87.50	125.00	0.48	99.52
70.00	12.50	46.12	100.00	4.33	91.83	140.00	0.48	100.00
75.00	7.12	53.37	105.00	2.88	94.71			
80.00	14.90	68.27	110.00	2.40	97.12			

Table 3: Data of polarization curves for corrosion of carbon steel at different concentrations of graft co-polymer nanoparticle in 1 M H_2SO_4 at temperature 293 K.

Inhibitor (mol)	**$-E_{cor}$ (mV)**	**I_{corr} (µA/cm^2)**	**β_a (mVdec^{-1})**	**$-\beta_c$ (mVdec^{-1})**	**Π%**	θ
balnk	*445.4*	*1940*	*70.3*	*93.0*	-	-
0.2	*386.0*	*543.2*	*51.5*	*105.8*	*72*	***0.72***
0.4	*383.9*	*406.5*	*34.3*	*49.2*	*79.04639*	***0.790464***
0.6	*396.6*	*263.4*	*38.3*	*88.8*	*86.42268*	***0.864227***
0.8	*402.5*	*135.4*	*33.3*	*103.2*	*93.02062*	***0.930206***

Surface Coverage

The extent of graft co-polymer nanoparticle on carbon steel s calculated via equation 4.

$\boldsymbol{\theta = \frac{\eta\%}{100}}$…….. (4) Where, θ : Surface coverage , η% : Inhibition efficiency .[33-35]

Potentiostatic Polarization Measurement

Potentiodynamic polarization measurements were used to test the corrosion inhibition efficiency (η%) of carbon steel by graft co-polymer nanoparticle in 1 M H_2SO_4. The experiments were carried out at temperature 293K , in presence of different concentrations of graft co-polymer nanoparticle (0.2, 0.4, 0.6, and 0.8 mol). Table (7) illustrates the measured parameters that include: corrosion potential (E_{corr}), corrosion current density (I_{corr}), cathodic Tafel slope (β_c) and anodic Tafel slope (β_a) , inhibition efficiency (η%) and surface coverage (θ). Table 3 explains using of graft co-polymer nanoparticle as a corrosion inhibitor, that leads to decrease in corrosion current density, as proportional relationship [36] with inhibition efficiency reacord 93% in the presence 0.8 mol of graft co-polymer nanoparticle (Figure 11)

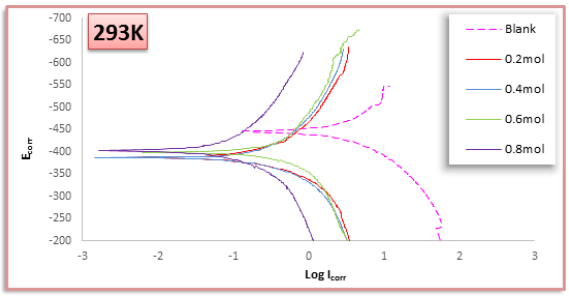

Figure 11: Potentiodynamic polarization curves for carbon steel in 1 M H_2SO_4 in the absence and presence of graft co-polymer nanoparticle at 293 K

Adsorption Isotherms

The adsorption of graft co-polymer nanoparticle on the alloy surface has been studied, the obtained results indicated that the adsorption obeys the Langmuir isotherms model (1) with correlation coefficients around (0.9947), From Langmuir equation the equilibrium constant of the adsorption process(K_{ads}) values were calculated, the values of free energy (ΔG_{ads}) and reaction enthalpy (ΔH_{ads}) were calculated according to equations (5-7) respectively. The entropy (ΔS_{ads}) was also calculated from the equation (8) (Figure 12) [37]

$$\frac{C_{inh}}{\theta} = \frac{1}{Kads} + C_{inh} \quad \text{……(5)}$$

$\Delta G_{ads} = -RT\ln(55{:}5\ K_{ads})$ ……..(6)

$$log\ K_{ads} = \left(\frac{-\Delta H_{ads}}{2.303RT}\right) + Constant \quad \text{…….. (7)}$$

$\Delta G = \Delta H - T\,\Delta S$ ……..(8)

where ΔG_{ads} is Gibbs free energy , ΔH_{ads} is enthalpy , ΔS_{ads} is entropy , T : temperature (K) , R : gas constant , C_{inh} : concentration (mol) of inhibitor , K_{ads} : adsorption constant .[38, 39]

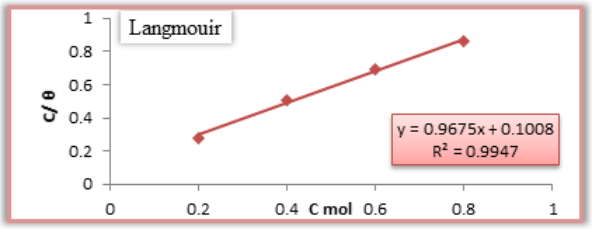

Figure 12: Langmuir relationship for graft co-polymer nanoparticle adsorption in 1M H_2SO_4 at 293 K.

Table 8: Thermodynamic parameters of graft co-polymer nanoparticle (1M H_2SO_4, 293K).

Temp. (k)	k_{ads} (mol^{-1})	ΔG (kj. mol^{-1})	ΔH (kj. mol^{-1})	ΔSkj.mol^{1}
293	9920635	-49.0282	-14.2709	0.118626

K_{ads} high value indicates a strong graft co-polymer nanoparticle adsorption on the metal surface, resulting in the creation of a protective layer that isolates the alloy's surface from the surrounding acidic medium.[40] Negative value for ΔH_{ads} , This indicates that the reaction is exothermic.[41] Negative G_{ads} value indicate that the adsorption of the graft co-polymer nanoparticle on the surface of the carbon steel alloy is a spontaneous reaction. It is reported that ΔG_{ads} value more than −40 kJ mol^{-1} indicate chemisorption (electron transfer between the orbitals of the inhibitor molecules and those of the metal to form co-ordinate bonding).[42-45]

Conclusion

The result of this study indicated that graft co-polymer nanoparticles that are used are efficient corrosion inhibitor. Also, as concentration of the retarder increases, density of the current corrosion reduces with increases of inhibition efficiency.

References

[1] N. Eliaz, Corrosion of metallic biomaterials: a review, Materials 12(3) (2019) 407.

[2] A. Kadhim, A. Al-Amiery, R. Alazawi, M. Al-Ghezi, R. Abass, Corrosion inhibitors. A review, International Journal of Corrosion and Scale Inhibition 10(1) (2021) 54-67.

[3] R. Rodrigues, S. Gaboreau, J. Gance, I. Ignatiadis, S. Betelu, Reinforced concrete structures: A review of corrosion mechanisms and advances in electrical methods for corrosion monitoring, Construction and Building Materials 269 (2021) 121240.

[4] R. Hsissou, Review on epoxy polymers and its composites as a potential anticorrosive coatings for carbon steel in 3.5% NaCl solution: Computational approaches, Journal of Molecular Liquids 336 (2021) 116307.

[5] F. Renner, A. Stierle, H. Dosch, D. Kolb, T.-L. Lee, J. Zegenhagen, Initial corrosion observed on the atomic scale, Nature 439(7077) (2006) 707-710.

[6] H.A. Ameen, K.S. Hassan, B.R. Mohameed, The effect of electroplating of Cr and Sn on corrosion resistance of low carbon steel (CK15)", American journal of scientific and industrial research (3) (2010) 565-572.

[7] B. Odio, E. Chinwuko, J. Chukwuneke, J. Sinebe, Investigation of the effect of corrosion on mild steel in five different environments, Int. J. Sci. Technol. Res 3 (2014) 306-310.

[8] H.H. Uhlig, R.W. Revie, Corrosion and corrosion control, (1985).

[9] N.A.A. K, The Combined Effect of Natural Inhibitors with Iodine Ion to Control Steel Corrosion in Acidic Medium, Diyala University - College of Science - Master Thesis (2018).

[10] D. Dwivedi, K. Lepková, T. Becker, Carbon steel corrosion: a review of key surface properties and characterization methods, RSC advances 7(8) (2017) 4580-4610.

[11] T.S.E. F.Missoum., Mémoire D'ingénieur d'Etat En Chimie Industrielle, Université d' Oran ((1996)) 10-15.

[12] T. Lanez, A. Rebiai, M.L. Belfar, Total polyphenol contents, radical scavenging and cyclic voltammetry of Algerian propolis, Int J Pharm Pharm Sci 6(1) (2014) 395-400.

[13] I. Obot, N. Obi-Egbedi, S. Umoren, Antifungal drugs as corrosion inhibitors for aluminium in 0.1 M HCl, Corrosion Science 51(8) (2009) 1868-1875.

[14] C.G. Dariva, A.F. Galio, Corrosion inhibitors–principles, mechanisms and applications, Developments in corrosion protection 16 (2014) 365-378.

[15] T. Ibrahim, M. AbouZour, Corrosion inhibition of mild steel using fig leaves extract in hydrochloric acid solution, (2011).

[16] R.S. Gouhar, E.F. Ewies, M.F. El-Shehry, M.N. Shaheen, E.M.M. Ibrahim, Synthesis and Utility of α, β-Unsaturated Ketone Bearing Naphthalene and Benzofuran Rings in the Synthesis of Some N-heterocycles with Their Antiviral and Antitumor Activity Evaluation, Journal of Heterocyclic Chemistry 55(10) (2018) 2368-2380.

[17] B. Ramaganthan, M. Gopiraman, L.O. Olasunkanmi, M.M. Kabanda, S. Yesudass, I. Bahadur, A.S. Adekunle, I.B. Obot, E.E. Ebenso,

Synthesized photo-cross-linking chalcones as novel corrosion inhibitors for mild steel in acidic medium: experimental, quantum chemical and Monte Carlo simulation studies, RSC advances 5(94) (2015) 76675-76688.
[18] R. Baskar, D. Kesavan, M. Gopiraman, K. Subramanian, Corrosion inhibition of mild steel in 1.0 M hydrochloric acid medium by new photo-cross-linkable polymers, Progress in Organic Coatings 77(4) (2014) 836-844.
[19] R. Baskar, M. Gopiraman, D. Kesavan, K. Subramanian, S. Gopalakrishnan, Utilization of photo-cross-linkable polymer for mild steel corrosion inhibition in 1.0 M HCl medium, Journal of Materials Engineering and Performance 24(8) (2015) 2847-2856.
[20] H. Eivaz Mohammadloo, S.M. Mirabedini, H. Pezeshk-Fallah, Microencapsulation of quinoline and cerium based inhibitors for smart coating application: Anti-corrosion, morphology and adhesion study, Progress in Organic Coatings 137 (2019) 105339.
[21] B. Fotovvati, N. Namdari, A. Dehghanghadikolaei, On coating techniques for surface protection: A review, Journal of Manufacturing and Materials processing 3(1) (2019) 28.
[22] E.F. Ewies, M. El-Hussieny, N.F. El-Sayed, M.M. Ali, A.E. Mahmoud, Synthesis, characterization, and antitumor evaluation of 4-aminoximidofurazan derivatives, Phosphorus, Sulfur, and Silicon and the Related Elements 191(7) (2016) 1000-1008.
[23] E.F. Ewies, M.F. El-Shehry, L.S. Boulos, Synthesis of some novel pyridazine derivatives of expected antitumor activity, Int. J. ChemTech Res 7 (2015) 2506.
[24] F. Cotting, I.V. Aoki, Smart protection provided by epoxy clear coating doped with polystyrene microcapsules containing silanol and Ce (III) ions as corrosion inhibitors, Surface and Coatings Technology 303 (2016) 310-318.
[25] X. Wang, H. Yang, F. Wang, Inhibition performance of a gemini surfactant and its co-adsorption effect with halides on mild steel in 0.25 M H2SO4 solution, Corrosion Science 55 (2012) 145-152.
[26] M. Hegazy, A. El-Tabei, H. Ahmed, Synthesis of nonionic surfactants and their inhibitive action on carbon steel in hydrochloric acid, Corrosion science 64 (2012) 115-125.
[27] H. Ashassi-Sorkhabi, N. Ghalebsaz-Jeddi, Inhibition effect of polyethylene glycol on the corrosion of carbon steel in sulphuric acid, Materials chemistry and physics 92(2-3) (2005) 480-486.
[28] B. Li, Y. Ouyang, Z. Haider, Y. Zhu, R. Qiu, S. Hu, H. Niu, Y. Zhang, M. Chen, One-step electrochemical deposition leading to superhydrophobic matrix for inhibiting abiotic and microbiologically influenced corrosion of Cu in seawater environment, Colloids and Surfaces A: Physicochemical and Engineering Aspects 616 (2021) 126337.
[29] D.L. Pavia, G.M. Lampman, G.S. Kriz, J.A. Vyvyan, Introduction to Spectroscopy, Cengage Learning2014.
[30] M.I. Choudhary, Applications of NMR Spectroscopy: Volume 9, Bentham Science Publishers2021.
[31] K. Takeyasu, Atomic Force Microscopy in Nanobiology, Jenny Stanford Publishing2016.
[32] B. Voigtländer, Atomic Force Microscopy, Springer International Publishing2019.
[33] O.J. Sanumi, The Study of Corrosion Inhibition of Polyethylene Glycol-Tyrosine Composite on Mild Steel in 1M HCl, University of Johannesburg (South Africa), 2019.
[34] M. Abdel-Goad, N. Mahmoud, B. Saad, The Analysis of Adsorption Phenomenon for Nano silica with Some Radionuclides Released in The Primary Coolant of PWR, Egyptian Journal of Chemistry 63(5) (2020) 1655-1667.
[35] S.S. Abd El Rehim, H.H. Hassan, M.A. Amin, Corrosion inhibition of aluminum by 1, 1 (lauryl amido) propyl ammonium chloride in HCl solution, Materials chemistry and physics 70(1) (2001) 64-72.
[36] A. Satapathy, G. Gunasekaran, S. Sahoo, K. Amit, P. Rodrigues, Corrosion inhibition by Justicia gendarussa plant extract in hydrochloric acid solution, Corrosion science 51(12) (2009) 2848-2856.
[37] G.A. Zhang, X.M. Hou, B.S. Hou, H.F. Liu, Benzimidazole derivatives as novel inhibitors for the corrosion of mild steel in acidic solution: Experimental and theoretical studies, Journal of Molecular Liquids 278 (2019) 413-427.
[38] H.I. Salman, S. Hassan, S.A. Abd-Alkareem, Inhibition Action of Non-polar Eichhornia crassipes Extract on the Carbon Steel Corrosion in 1 M HCl, Macromolecular Symposia, Wiley Online Library, 2022, p. 2100304.
[39] H.E. Salman, A.A. Balakit, M.A.A.H. Allah, Study of the corrosion inhibitive effect and adsorption process of two azo-aldehydes on carbon steel in 1 M H2SO4, IOP Conference Series: Materials Science and Engineering, IOP Publishing, 2019, p. 012078.
[40] M.A. Albo Hay Allah, A.A. Balakit, H.I. Salman, A.A. Abdulridha, Y. Sert, New heterocyclic compound as carbon steel corrosion inhibitor in 1 M H2SO4, high efficiency at low concentration: Experimental and theoretical studies, Journal of Adhesion Science and Technology (2022) 1-23.

[41] C. Verma, M. Quraishi, A. Singh, 2-Amino-5-nitro-4, 6-diarylcyclohex-1-ene-1, 3, 3-tricarbonitriles as new and effective corrosion inhibitors for mild steel in 1 M HCl: Experimental and theoretical studies, Journal of Molecular Liquids 212 (2015) 804-812.
[42] M. Alfakeer, M. Abdallah, A. Fawzy, Corrosion inhibition effect of expired ampicillin and flucloxacillin drugs for mild steel in aqueous acidic medium, Int. J. Electrochem. Sci 15 (2020) 3283-3297.

[43] Abood, Emad Salaam, Ahmed Salim Abed, and Zahara Njah Salman. "New Fe2O3 Nanoparticles Modified Carbon Paste Electrode: A Cyclic Voltammetric Study." Egyptian Journal of Chemistry 64.12 (2021): 7409-7415.
[44] Amer Mousa Jouda, Emad Salaam Abood, and Mothana Salih Mashloor, Copper Metal at New CuO Nanoparticles Modified Carbonpaste Electrode: Selective Voltammetric Determination. Nano Biomed. Eng., 2018, 10(3): 243-249.
[45] Abood, E. S., et al. "Zinc oxide and Zinc oxide Nanoparticles Carbon Past Ion Selective Electrode: A Cyclic Voltammetry Comparison Study." Journal of Physics: Conference Series. Vol. 2047. No. 1. IOP Publishing, 2021.